FUDMA Journal of Sciences (FJS)
ISSN online: 2616-1370
ISSN print: 2645 - 2944
Vol. 10 No. 4, February, 2026, pp 343 – 355
DOI: https://doi.org/10.33003/fjs-2026-1004-4626

VALORIZATION OF AVOCADO SEED RESIDUE AS BIOMASS FOR BIOSYNGAS PRODUCTION VIA OPTIMIZED STEAM GASIFICATION PROCESS USING BOX-BEHNKEN DESIGN (BBD) APPROACH

[*1]Jibrin Mohammed, [2]Kabiru S. Madaki and [3]Jafar A. Ibrahim

[1]Department of Chemistry, Faculty of Natural & Applied Sciences, Nasarawa State University, Keffi, Nasarawa State, Nigeria.
[2]Department of Science and Laboratory Technology, Faculty of Natural & Applied Sciences, Nasarawa State University, Keffi, Nasarawa State, Nigeria.
[3]Department of Science and Laboratory Technology, College of Agriculture, Science Lafia, Nasarawa State, Nigeria.

Corresponding Author's Email: jibrinmohammed@nsuk.edu.ng

ABSTRACT

Sustainable conversion of agricultural residues into renewable fuels is critical for addressing global energy and environmental challenges. This study investigates the potential of avocado seed residue (ASR), a lignocellulosic by-product of oil extraction, as a feedstock for biosyngas production via optimized steam gasification using Box-Behnken design (bbd) approach**.**The physicochemical and elemental compositions of ASR were assessed using standard analytical procedures, which revealed favorable properties for biosyngas production. Gasification experiments were conducted in a laboratory-scale bubbling fluidized bed reactor, and process optimization was performed using the Box-Behnken Design approach. The effects of temperature, steam-to-biomass ratio (S/B), and particle size on hydrogen (H_2), carbon monoxide (CO), and methane (CH_4) yields were systematically analyzed and indicated a strong influence on the yields. Analysis of variance (ANOVA) confirmed the significance and predictive accuracy of the quadratic models ($p < 0.0001$, $R^2 > 0.97$). Maximum yields of 30.76 vol% H_2, 11.35 vol% CO, and 11.00 vol% CH_4 were achieved at 900 °C, S/B ratio of 0.6, and particle size of 2.5 mm, with a very close agreement between predicted and experimental values (deviation <2%), which further confirms the reliability of the developed models. The findings demonstrated that ASR is a promising feedstock for efficient biosyngas generation, and that RSM-BBD provides a reliable technique for optimizing gasification parameters for maximum yield of biosyngas from the avocado seed residue.

Keywords: Avocado Seed Residue, Optimization, Steam Gasification, Biosyngas, BBD

INTRODUCTION

Access to clean, reliable, and affordable energy remains a critical objective for both developed and developing nations worldwide. Despite this goal, fossil fuels still dominate the global energy mix, accounting for nearly 85% of total energy demand (Bayetero *et al.*, 2022). This persistent dependence on finite resources raises concerns regarding long-term energy security and significantly contributes to environmental degradation (Naveenkumar and Baskar, 2021). The large-scale combustion of fossil fuels releases substantial quantities of greenhouse gases, particularly carbon dioxide (CO_2), which are major drivers of global warming and climate change. Simultaneously, a growing population, industrialization, and economic expansion continue to increase global energy consumption, further intensifying carbon emissions (Thomson *et al.*, 2020;Savannah, 2021).

In light of these challenges, increasing attention has been directed toward the development and utilization of renewable energy resources**,** with biomass emerging as a promising and sustainable alternative (Marwan *et al*., 2021; Sharma *et al.*, 2021). Biomass-based energy systems offer dual advantages by contributing to greenhouse gas mitigation while simultaneously supporting effective waste management strategies, especially in developing countries like Nigeria (Ezealigo *et al.*, 2021; Savannah, 2021). In addition, the transition from fossil fuels to biomass and other renewable energy sources has been shown to enhance energy affordability and environmental sustainability (Abdullah *et al.*, 2019; Adeyemi *et al.*, 2020). Biomass can be efficiently exploited through three primary pathways: thermal applications (heating and cooling), electricity generation, and transportation fuels (Bijoy *et al.*, 2020; Muhammad *et al.*, 2020). Consequently, several developed nations have expanded the integration of biomass into their energy portfolios as part of broader efforts to reduce fossil fuel dependence and limit greenhouse gas emissions (Antonio *et al.*, 2018).

Avocado (*Persea americana*) is a tropical fruit tree that reaches a height of 5-15 m. The fruit varies considerably in size, weighing approximately 120 g to 2.5 kg, and generally requires 5-15 months to reach maturity (Minerva *et al.*, 2020). Unlike many fruits, avocado ripens after harvest rather than on the tree. Both the pulp and the seed contain appreciable amounts of oil, and the fruit is nutritionally valuable, providing essential fatty acids, proteins, minerals, and vitamins such as A, B6, C, D, and E (Chel-Guerrero *et al.*, 2016). Global demand for avocado, whether consumed fresh or processed into products such as oil and paste, has increased substantially in recent years (Minerva *et al.*, 2020). This growing market has encouraged many countries to expand avocado cultivation and industrial processing. However, large-scale production also generates significant quantities of residual biomass in the form of waste, including peels, seeds, pruning residues, and by-products from oil extraction (Marcos *et al.*, 2019; Minerva *et al.*, 2020). These materials represent an underutilized resource with potential for conversion into valuable co-products such as biosyngas. Effective valorization, however, requires improved resource management strategies, optimized processing systems, and integrated production approaches to ensure efficient and sustainable utilization (Minerva *et al.*, 2020).

Biosyngas refers to synthesis gas derived from biomass and is chemically comparable to syngas produced from natural gas or other fossil-based resources (Chinedu *et al.*, 2020). The production of biosyngas is regarded as a relatively straightforward and integrated process, involving a low

degree of organic transformation, typically in the range of 5-10 wt.%**,** depending on the type of biomass feedstock and the operating conditions employed (Gagliano *et al.,* 2017; Prakash *et al.,* 2022). Biomass can be converted to biosyngas through physicochemical, biochemical, and thermochemical pathways, all of which are considered environmentally sustainable options (Sezer & Ozveren, 2021).

Gasification is a thermochemical conversion process that transforms biomass into biosyngas under sub-stoichiometric conditions, achieving a high level of carbon conversion (Ajorloo *et al.,* 2022). Owing to the inherent complexity of the gasification process, where multiple variables such as biomass type, operating temperature and pressure, feedstock particle size, bed material characteristics, gasifying agent, equivalence ratio (ER), and steam-to-biomass (S/B) ratio simultaneously influence product yield and composition, process modelling and optimization are essential (Solal *et al.,* 2022; Font, 2023)**.**

In this regard, the application of response surface methodology (RSM) provides an effective and systematic approach for evaluating the combined effects of these parameters and optimizing biosyngas production. Response Surface Methodology (RSM) is a collection of statistical and mathematical tools employed for the modeling, analysis, and optimization of processes in which the response variables are influenced by several independent factors (Jibrin *et al.,* 2025; Abubakar *et al*., 2026). Compared with extensive experimental trials, RSM offers a cost-effective and time-efficient approach for predicting gaseous fuel characteristics, thereby reducing experimental effort and resource consumption (Halim *et al.,* 2019; Inayat *et al.,* 2020). In the present study, the Box-Behnken Design (BBD)**,** integrated within the RSM framework, was applied to examine the interactive effects of operating temperature, biomass particle size, and steam-to-biomass (S/B) ratio on biosyngas yield.

Despite the extensive availability of literature on biomass gasification, no previous study has reported the application of Box-Behnken Design to the gasification of avocado seed residue as by product for biosyngas production**.** Consequently, the objective of this research is to assess the suitability of avocado seed residue as a feedstock for biosyngas generation and to optimize key process parameters using BBD to maximize biosyngas yield.

MATERIALS AND METHODS

Sample Collection and Preparation

The avocado residue was obtained as a by-product after extracting oil from the raw seeds using a Soxhlet extractor. To eliminate any traces of n-hexane solvent used during extraction, the sample was thoroughly rinsed with hot water. It was then sun-dried for two weeks, followed by oven-drying at 105 ℃ for 24 h to ensure the removal of residual moisture. The dried material was finely ground and sieved into three particle sizes: 1.5 mm, 2.5 mm, and 3.5 mm.

Physicochemical and Ultimate Analyses

Proximate parameters, including ash content, moisture, fixed carbon, and volatile matter, were determined using standard analytical methods (ASTM E-3173, 3174, and 3175) as described in the literature (Sango *et al.,* 2018; Preeti *et al.,* 2024). Lignocellulosic components were quantified following the method of Betene *et al.* (2020), with minor modifications. Ultimate analysis was performed using an EMA 502 Elemental Analyzer (CHNS-O) in accordance with the ASTM D5373-16 standard procedure (Varank *et al.,* 2021).

Experimental Design

The experimental setup was designed using the Box-Behnken Design (BBD) within the Response Surface Methodology (RSM) framework, implemented through Design Expert version 13. Three operating parameters; gasification temperature, steam-to-biomass ratio (S/B), and biomass particle size were selected as independent variables. Each factor was evaluated at three coded levels (-1, 0, +1), resulting in 17 experimental runs, including five replicates at the center point to assess experimental error and model adequacy.The response variables were defined as the volumetric yields of hydrogen (H_2), carbon monoxide (CO), and methane (CH_4), consistent with methodologies reported in related gasification studies (Umar *et al.,* 2021; Varank *et al*., 2021).

Gasification Experiment

The gasification trials were performed using a laboratory-scale bubbling fluidized bed gasifier fabricated from stainless steel. The reactor had an internal diameter of 70 mm and a height of 950 mm. Silica sand was employed as the bed material owing to its high thermal stability and excellent heat retention capacity, which facilitate uniform temperature distribution and stable high-temperature operation (Halim *et al.,* 2019).The system was integrated with an electric furnace to ensure accurate temperature regulation, a controlled biomass feeding unit, a steam generation system, and a gas cleaning section connected to a gas analyzer interfaced with a computer for real-time monitoring. Prior to each experiment, the reactor temperature was gradually raised in stages until the predetermined operating temperature was attained and stabilized. Once thermal equilibrium was achieved, the reactor was briefly opened to introduce the prepared biomass sample, after which it was immediately sealed to commence the gasification process.Experiments were conducted under different operating conditions as specified by the Box-Behnken Design (BBD) matrix (Table 1). The produced gas stream was continuously analyzed, with data transmitted to the computer via a LAN-based connection to the gas analyzer. Gas composition measurements were recorded automatically at one-second intervals and stored digitally for subsequent analysis. Upon completion of each experimental run, the gasifier was switched off and allowed to cool to ambient temperature before the remaining char and ash residues were collected for further evaluation.

Table 1: Box-Behnken Design (BBD) with Coded and Actual Values of Experimental Parameters of the Design Matrix used in Production of Biosyngas from the Seed Residue

Parameters	Symbols	-1	0	+1
Temperature (°C)	A	700	800	900
Steam/biomass ratio	B	0.2	0.4	0.6
Particle size (mm)	C	1.5	2.5	3.5

Statistical Analysis

Analysis of variance (ANOVA) was employed as the primary statistical tool to evaluate the effects of process variables and their interactions on the response outputs. The assessment involved three main statistical tests: the lack-of-fit test, the regression model analysis, and the evaluation of the significance of individual model terms. Based on these analyses, a second-order polynomial equation was developed

to represent the experimental conditions and predict the response values, as presented in Equation (1)(Umar *et al.,* 2021).

$$Y= \beta_0\sum_{i=1}^{k}\beta_i x_i + \beta_0\sum_{i=1}^{k}\beta_{ii}x_i^2 + \sum_{1\le i\le j}^{k}\beta_{ij}x_i x_j + C \quad (1)$$

Where, where Y is the response (%); 0, i, ii, and ij are the intercept, linear, quadratic, and interaction coefficients, respectively, while Xi and Xj are the independent factors

RESULTS AND DISCUSSION

Physicochemical and Elemental Analyses of Avocado Seeds Residue (ASR)

The proximate and ultimate characteristics of avocado seed residue (Table 2) demonstrated its strong potential as a feedstock for thermochemical conversion to biosyngas. Low moisture is advantageous for gasification since it reduces drying energy demand and minimizes energy losses during thermal conversion (Serrano *et al*., 2011).The moisture content (4.69 ± 0.14%) obtained from this study falls below the typical 15% threshold recommended for efficient gasification, which limits the need for extensive pre-drying and reducing associated energy losses. Volatile matter plays a key role in achieving high gasification yields since it directly contributes to the release of combustible gases such as CO, H_2, and CH_4 (Preeti *et al.,* 2024). The relatively high volatile matter content (47.28 ± 2.10%) suggests enhanced devolatilization during pyrolysis and the early stages of gasification. High volatile fractions are generally associated with increased formation of primary gaseous products such as CO, H_2, and CH_4, contributing to improved cold gas efficiency and stable reactor operation (Hamad *et al.,* 2016; Aqsha *et al.,* 2017).

The fixed carbon content (37.20 ± 0.45%) is significant and plays a crucial role in sustaining secondary char gasification reactions (Wang *et al.,* 2015). Heterogeneous reactions, including the Boudouard reaction ($C + CO_2 \rightarrow 2CO$) and steam gasification ($C + H_2O \rightarrow CO + H_2$), are facilitated by adequate fixed carbon levels, thereby enhancing syngas yield (Ajorloo *et al.,* 2022). The balanced proportion of volatile matter to fixed carbon indicates that ASR can support both rapid gas release and sustained char conversion, promoting overall process efficiency (Gillespie *et al*., 2013). In addition, the low ash content (3.83 ± 0.23%) is advantageous for high-temperature applications, as it reduces the likelihood of slagging, fouling, and bed agglomeration (Preeti *et al.,* 2024). Lower mineral content also minimizes risks of catalyst deactivation and reactor corrosion, improving operational stability (Antonio *et al*., 2018).

The lignicellulose composition plays a critical role in determining decomposition behavior and the quality of syngas produced (Bychkov *et al.,* 2014; Anukam *et al.,* 2016).This study shows that ASR is rich in hemicellulose (42.35 ± 0.87%), followed by lignin (21.75 ± 2.46%) and cellulose (15.50 ± 1.28%). A high hemicellulose fraction favors early-stage thermal decomposition and enhanced volatile release, while lignin contributes to char formation and promotes secondary reforming reactions that can increase hydrogen production (Preeti *et al.,* 2024). This lignocellulosic distribution supports staged thermal degradation and sustained gas evolution during conversion (Bychkov *et al.,* 2014; Aqsha *et al.,* 2017).

Ultimate analysis further confirms the energetic suitability of ASR. The carbon content (50.22 ± 1.17%) is relatively high, supporting CO generation and contributing to an improved calorific value. The hydrogen fraction (5.20 ± 0.11%) enhances the potential for hydrogen formation through steam reforming and water-gas shift reactions (Bychkov *et al.,* 2017; Seçer & Hasanoglu, 2020). Although the oxygen content (40.93 ± 3.02%) is typical of lignocellulosic materials and may slightly reduce energy density, the presence of oxygenated functional groups improves thermal reactivity by facilitating bond cleavage during gasification (Antonio *et al*., 2018).

Based on Dulong's empirical equation, the higher heating value (HHV) of ASR was estimated to be approximately 17.09 MJ/kg. This value is comparable to that of many agricultural residues and confirms that ASR possesses sufficient energy content for effective thermochemical processing (Singh *et al*., 2013; Danish *et al.,* 2015; Wang *et al*., 2020). The combination of moderate HHV, high volatile matter, and substantial fixed carbon suggests strong potential for efficient biosyngas production with favorable cold gas efficiency (Wang *et al*., 2020).

Furthermore, the nitrogen (0.65 ± 0.01%) and sulfur (0.02 ± 0.00%) contents are extremely low, which significantly reduces the formation of nitrogen- and sulfur-based pollutants such as NOx and SOx during gasification.This characteristic enhances the environmental performance of ASR-derived syngas and decreases the extent of downstream gas purification required (Seçer & Hasanoglu, 2020).

Table 2: Physicochemical and Elemental Compositions of Avocado Seeds Residue (ASR)

Physicochemical component	Composition(%)
Moisture	4.69 ± 0.14
Ash	3.83 ± 0.23
Fixed carbon	37.20 ± 0.45
Volatile M.	47.28 ± 2.10
Cellulose	15.50 ±1.28
hemicellulose	42.35 ± 0.87
Lignin	21.75 ± 2.46
Ultimate Analysis	
Carbon (C)	50.22±1.17
Hydrogen (H)	5.20 ± 0.11
Oxygen (O)	40.93 ± 3.02
Nitrogen (N)	0.65± 0.01
Sulphur (S)	0.02 ± 0.00
Calorific value(MJ/kg)	17.09± 0.01

Response Data Analysis of Biosyngas Produced from ASR

The experimental and model-predicted results for biosyngas production from avocado seed residue (ASR) revealed notable variations across the operating conditions investigated (Table 3). Hydrogen yield ranged from 10.65 vol% (Run 6: 900 °C, S/B = 0.4, particle size = 1.5 mm) to 30.76 vol% (Run 4: 900 °C, S/B = 0.6, particle size = 2.5 mm). From the results, the elevated temperatures coupled with higher steam-to-biomass ratios significantly enhanced hydrogen generation. For example, at 900 °C, increasing the S/B ratio from 0.2 to 0.6 resulted in an increase in hydrogen yield from 24.00 vol% to 30.76 vol%. Conversely, lower temperatures, such as 700 °C (Run 3: S/B = 0.6), limited hydrogen formation due to insufficient thermal energy to drive gasification reactions and the water-gas shift equilibrium effectively (Seçer & Hasanoglu, 2020; Ajorloo *et al*., 2022).

Carbon monoxide concentrations varied between 5.63 vol% (Run 10: 800 °C, S/B = 0.6, particle size = 1.5 mm) and 20.00 vol% (Run 8: 900 °C, S/B = 0.4, particle size = 3.5 mm). CO production was generally promoted at higher temperatures and moderate steam input, particularly with larger particle sizes. However, excessive steam levels reduced CO concentration by shifting the water–gas shift reaction toward hydrogen formation (Ajorloo *et al*., 2022). Notably, Run 8 exhibited the highest CO yield despite a comparatively lower hydrogen concentration, indicating that CO formation was more strongly influenced by particle size and thermal conditions than by steam content alone.

Methane yield ranged from 2.00 vol% (Run 12: 800 °C, S/B = 0.6, particle size = 3.5 mm) to 15.02 vol% (Run 17: 800 °C, S/B = 0.4, particle size = 2.5 mm). The highest CH_4 concentrations were observed at intermediate temperatures and moderate steam-to-biomass ratios with a particle size of 2.5 mm, suggesting that methanation reactions are favored under mid-range operating conditions. At higher temperatures, methane yield declined due to thermal cracking and reforming reactions (Font, 2023). For instance, increasing the temperature from 800 °C (Run 2) to 900 °C (Run 6) led to a reduction in methane concentration from 14.00 vol% to 13.00 vol%.

However, hydrogen emerged as the dominant syngas component, reaching a maximum of 30.76 vol%, followed by carbon monoxide (20.00 vol%) and methane (15.02 vol%). These values exceed the approximately 17.5 vol% hydrogen and carbon monoxide and 5.3 vol% methane reported in kinetic modeling studies of biomass gasification by Bijoy *et al.* (2020), although lower than the combined 98.42 vol% H_2 + CO reported in optimized coal gasification systems using Taguchi and RSM techniques (Hou & Zhang, 2017). The variation in gas composition can be attributed to differences in feedstock characteristics and operational parameters.

Furthermore, statistical evaluation using ANOVA confirmed that the quadratic regression models for hydrogen (H_2), carbon monoxide (CO), and methane (CH_4) were all statistically significant ($p < 0.0001$), indicating that the quadratic formulations effectively represented the experimental responses. Among the three responses, the methane model exhibited the highest statistical strength, with an F-value of 119.07, followed by the carbon monoxide model (F = 45.97) and the hydrogen model (F = 37.69). The high F-values and very low probability levels confirm that the developed models are statistically reliable and suitable for predicting biosyngas composition under the studied conditions.

The coefficients of determination (R^2) were 0.9798 for H_2, 0.9834 for CO, and 0.9798 for CH_4, demonstrating that more than 97% of the variability in the responses was explained by the models. The adjusted R^2 values (0.9538 for H_2, 0.9620 for CO, and 0.9798 for CH_4) further indicate strong model consistency after accounting for the number of predictors. Similarly, the predicted R^2 values (0.8850 for H_2, 0.8782 for CO, and 0.8850 for CH_4) show good agreement between experimental observations and model predictions, confirming adequate external predictability.

The CH_4 model displayed the lowest standard deviation (0.6214), reflecting minimal residual dispersion and improved precision. In contrast, the CO model recorded the lowest coefficient of variation (5.27%) and the highest adequate precision value (28.83), indicating excellent reproducibility and a strong signal-to-noise ratio. Although the hydrogen model also demonstrated satisfactory statistical performance, its R^2 and adequate precision values were marginally lower compared to those of CO and CH_4. The statistical indicators confirm that the developed models are robust and consistent with similar regression-based gasification studies reported in the literature (Shahbaz *et al*., 2016; Inayat *et al.,* 2019).

Figures 1-3 present the correlation between the experimental measurements and the model-predicted values for H_2, CO, and CH_4. In each case, the plotted data points align closely along the reference line, indicating strong agreement between observed and estimated responses. This graphical confirmation supports the high coefficients of determination (R^2) obtained from ANOVA (H_2: 0.9798; CO:0.9834; CH_4: 0.9935). Furthermore, the small residual deviations and statistically insignificant lack-of-fit results demonstrate that the developed quadratic models provide an accurate and reliable representation of biosyngas production from avocado seed residue.The second-order polynomial regression models generated for hydrogen, carbon monoxide, and methane are expressed in Equations (2)-(4), respectively:

$$H_2\ (vol\%) = 24.244 + 6.625A + 0.74625B + 2.25AB - 3.82075B^2 - 7.06075C^2 \quad (2)$$

$$CO\ (vol\%) = 13.026 + 2.08A - 2.04625B + 1.31625C - 1.4325AB + 1.3225AC + 2.817A^2 - 3.4005B^2 \quad (3)$$

$$CH_4\ (vol\%) = 14.406 + 3.40625A - 0.625B - 0.71875C - 1.9975AC - 5.57925B^2 - 5.82675C^2 \quad (4)$$

In these equations, positive regression coefficients indicate that increasing the corresponding variable enhances the syngas yield, whereas negative coefficients imply a reduction in yield with increasing parameter values. Only statistically significant terms were retained in the final models to ensure predictive reliability.

To further assess the influence of individual factors, perturbation plots (Figures 4-6) were analyzed. For hydrogen production (Figure 4), temperature (A) exhibited the steepest slope, confirming its dominant effect, followed by the steam-to-biomass ratio (B) and particle size (C), which exerted comparatively moderate influences. This observation is consistent with ANOVA findings, where temperature recorded the highest F-value (F = 174.67), highlighting its statistical significance.

In the case of carbon monoxide (Figure 5), both temperature and steam-to-biomass ratio demonstrated strong and highly significant effects ($p < 0.0001$), while particle size showed a less pronounced but still measurable impact. For methane production (Figure 6), temperature again emerged as the most influential factor, followed by particle size. The curvature observed in the particle size profile confirms the statistical significance of its quadratic term (C^2, $p < 0.0001$). Conversely, the steam-to-biomass ratio exhibited only a minor effect on methane yield.

ANOVA results further substantiated these trends. Hydrogen formation was predominantly governed by temperature, whereas carbon monoxide and methane production were influenced by all three process variables; temperature, steam-to-biomass ratio, and particle size albeit to different extents. These findings indicate that hydrogen generation is primarily temperature-dependent, while CO and CH_4 yields are controlled by combined thermal and mass-transfer effects associated with the operating parameters.

The interaction effects of the operating variables were examined using contour plots (Figures 7-9), which illustrated the combined influence of two parameters while maintaining the third at a constant level.For hydrogen production (Figure 7), the highest yields were observed at elevated temperatures (approximately 900 °C) and higher steam-to-biomass ratios (around 0.6). This behavior can be attributed to enhanced steam reforming and water-gas shift reactions at higher thermal conditions (Bijoy *et al*., 2020). Additionally, smaller particle sizes contributed to increased hydrogen yield under these conditions, likely due to improved heat transfer and greater surface area, which enhance reaction kinetics and biomass conversion efficiency.

In the case of carbon monoxide (Figure 8), CO concentration increased with temperature but decreased at higher steam-to-biomass ratios. This trend aligns with the water-gas shift reaction, in which CO is consumed to produce hydrogen in the presence of excess steam. Maximum CO production was achieved at high temperatures combined with moderate to larger particle sizes, suggesting that thermal intensity and residence characteristics play a key role in CO formation.

Methane production (Figure 9) exhibited a different pattern, with peak yields occurring at approximately 800 °C and a moderate steam-to-biomass ratio of about 0.4. Particle size also significantly influenced CH_4 formation, with intermediate sizes (around 2.5 mm) favoring higher methane concentrations. Extremely fine particles may promote secondary cracking reactions, while larger particles can introduce heat and mass transfer limitations, both of which reduce methane yield (Font, 2023). The statistically significant interaction between temperature and particle size (AC term, $p = 0.0004$) further highlights the importance of their combined influence on methane formation.

Optimization of the process variables was performed using the numerical desirability function within the Box-Behnken Design approach. The optimal gasification conditions were identified as 800 °C, a steam-to-biomass ratio of 0.60, and a particle size of 2.5 mm. Under these optimized conditions, the model predicted yields of 30.89 vol% H_2, 20.26 vol% CO, and 14.08 vol% CH_4. Experimental validation conducted at the same operating parameters produced average concentrations of 31.01 vol% H_2, 20.63 vol% CO, and 14.16 vol% CH_4, corresponding to relative deviations of 0.39%, 1.83%, and 0.57%, respectively.

The close agreement between predicted and experimental results, with all deviations below 2%, confirms the efficacy of the developed models and validates the applicability of the BBD approach for optimizing biosyngas production from avocado seed residue.

Table 3: Experimental Design (Bbd) Matrix and the Actual and Predicted Performance Index Values of the Syngas Composition Produced from Avocado Seed Residue

	Variables			H_2		CO		CH_4	
No. runs	Temp.(ºC)	S/B	PS (mm)	Exp. values (%)	Model Values (%)	Exp. values (%)	Model values (%)	Exp. values (%)	Model values (%)
1	700	0.2	2.5	15.40	16.43	10.67	10.98	5.00	5.22
2	800	0.2	2.5	24.00	24.38	18.11	18.00	14.00	12.53
3	700	0.6	2.5	13.00	12.62	9.64	9.75	4.00	4.47
4	900	0.6	2.5	30.76	30.37	11.35	11.04	11.00	10.78
5	700	0.4	1.5	27.00	24.24	13.00	13.10	3.88	3.32
6	900	0.4	1.5	10.65	11.24	14.10	14.62	13.00	14.13
7	700	0.4	3.5	21.26	21.68	13.61	13.03	6.00	5.87
8	900	0.4	3.5	12.00	11.79	20.00	19.90	8.13	8.69
9	800	0.2	1.5	15.45	16.43	10.28	9.87	4.00	4.34
10	800	0.6	1.5	14.00	13.02	5.63	5.42	3.00	3.09
11	800	0.2	3.5	12.00	12.21	11.93	12.14	3.00	2.91
12	800	0.6	3.5	22.91	24.24	8.00	8.41	2.00	1.66
13	800	0.4	2.5	27.00	26.41	13.04	13.03	14.00	14.41
14	800	0.4	2.5	23.77	24.24	13.30	13.03	14.00	14.41
15	800	0.4	2.5	23.77	24.24	13.30	13.03	14.00	14.41
16	800	0.4	2.5	23.77	24.24	13.61	13.03	15.01	14.41
17	800	0.4	2.5	23.77	24.24	11.88	13.03	15.02	14.41

Note: S/B = steam to biomass ratio; PS= particle size

Table 4: ANOVA Results and Fit Statistics Obtained from the Quadratic Model for H_2 Produced from the Avocado Seed Residue

Source	Sum of Squares	DF	Mean Square	F-value	p-value	
Model	681.98	9	75.78	37.69	< 0.0001	Significant
A-A	351.13	1	351.13	174.67	< 0.0001	
B-B	4.46	1	4.46	2.22	0.1802	
C-C	7.35	1	7.35	3.66	0.0974	
AB	20.25	1	20.25	10.07	0.0156	
AC	6.92	1	6.92	3.44	0.1060	
BC	7.43	1	7.43	3.69	0.0961	
A^2	0.4495	1	0.4495	0.2236	0.6507	

Source	Sum of Squares	DF	Mean Square	F-value	p-value	
B^2	61.47	1	61.47	30.58	0.0009	
C^2	209.91	1	209.91	104.42	< 0.0001	
Residual	14.07	7	2.01			
Lack of Fit	4.02	3	1.34	0.5337	0.6834	Not significant
Pure Error	10.05	4	2.51			
Cor Total	696.05	16				
SD	1.42					
Mean	19.28					
CV%	7.35					
R^2	0.9798					
Adjusted R^2	0.9538					
Predicted R^2	0.8850					
AP	18.2473					

Note: A = temperature; B=steam to biomass ratio; C= particle size; SD= standard deviation;CV =coefficient of variation; AP =average precision

Table 5: ANOVA Results and Fit Statistics Obtained from the Quadratic Model for CO Produced from the Avocado Seed Residue

Source	Sum of Squares	DF	Mean Square	F-value	p-value	
Model	177.44	9	19.72	45.97	< 0.0001	Significant
A-A	34.61	1	34.61	80.70	< 0.0001	
B-B	33.50	1	33.50	78.10	< 0.0001	
C-C	13.86	1	13.86	32.32	0.0007	
AB	8.21	1	8.21	19.14	0.0033	
AC	7.00	1	7.00	16.31	0.0049	
BC	0.1296	1	0.1296	0.3022	0.5996	
A^2	33.41	1	33.41	77.91	< 0.0001	
B^2	48.69	1	48.69	113.52	< 0.0001	
C^2	1.86	1	1.86	4.35	0.0755	
Residual	3.00	7	0.4289			
Lack of Fit	1.20	3	0.3992	0.8847	0.5209	Not significant
Pure Error	1.80	4	0.4512			
Cor Total	180.44	16				
SD	0.6549					
Mean	12.44					
CV%	5.27					
R^2	0.9834					
Adjusted R^2	0.9620					
Predicted R^2	0.8782					
AP	28.8260					

Note: A = temperature; B=steam to biomass ratio; C= particle size; SD= standard deviation;CV =coefficient of variation; AP =average precision

Table 6: ANOVA Results and Fit Statistics Obtained from the Quadratic Model for CH_4 Produced from the Avocado Seed Residue

Source	Sum of Squares	DF	Mean Square	F-value	p-value	
Model	411.72	9	45.75	119.07	< 0.0001	Significant
A-A	92.82	1	92.82	241.59	< 0.0001	
B-B	3.13	1	3.13	8.13	0.0246	
C-C	4.13	1	4.13	10.76	0.0135	
AB	0.2500	1	0.2500	0.6507	0.4464	
AC	15.96	1	15.96	41.54	0.0004	
BC	0.0000	1	0.0000	0.0000	1.0000	
A^2	1.40	1	1.40	3.65	0.0979	
B^2	131.07	1	131.07	341.13	< 0.0001	
C^2	142.95	1	142.95	372.07	< 0.0001	
Residual	2.69	7	0.3842			
Lack of Fit	1.45	3	0.4844	1.57	0.3290	Not significant
Pure Error	1.24	4	0.3091			
Cor Total	414.41	16				
SD	1.42					
Mean	19.28					
CV%	7.35					
R^2	0.9798					
Adjusted R^2	0.9538					

Source	Sum of Squares	DF	Mean Square	F-value	p-value
Predicted R^2	0.8850				
AP	18.2473				

Note: A = temperature; B=steam to biomass ratio; C= particle size; SD= standard deviation;CV =coefficient of variation; AP =average precision

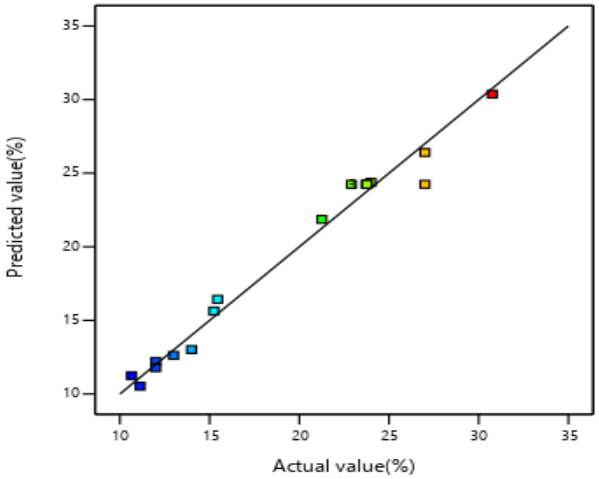

Figure 1: Plot of Actual against Predicted Volume of H_2 Gas Produced from Avocado Seed Residue

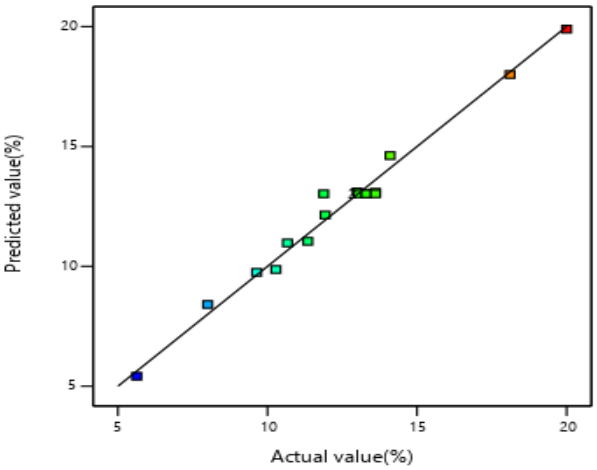

Figure 2: Plot of Actual against Predicted Volume of CO Gas Produced from Avocado Seed Residue

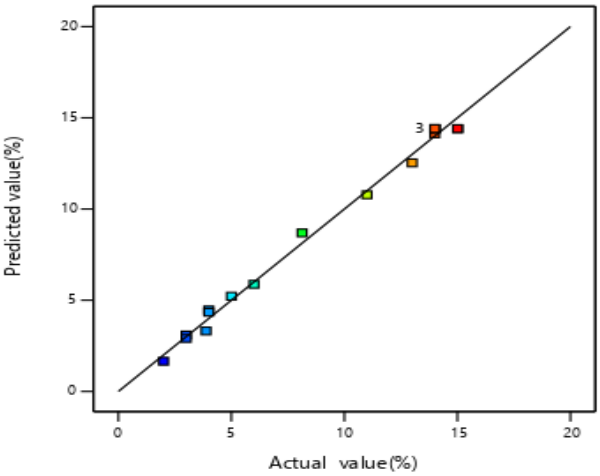

Figure 3: Plot of Actual against Predicted Volume of CH_4 Produced from Avocado Seed Residue

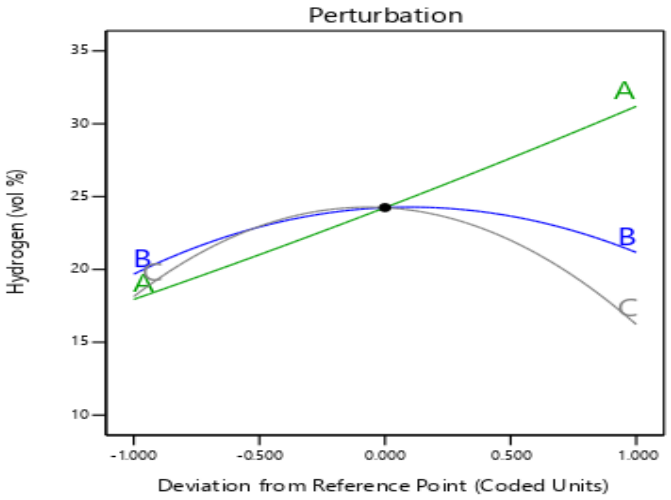

Figure 4: Perturbation Plots of Model Terms Effects of (A; Temperature, B; S/B Ratio, and C; Particle Size for H_2 Produced from Avocado Seed Residue

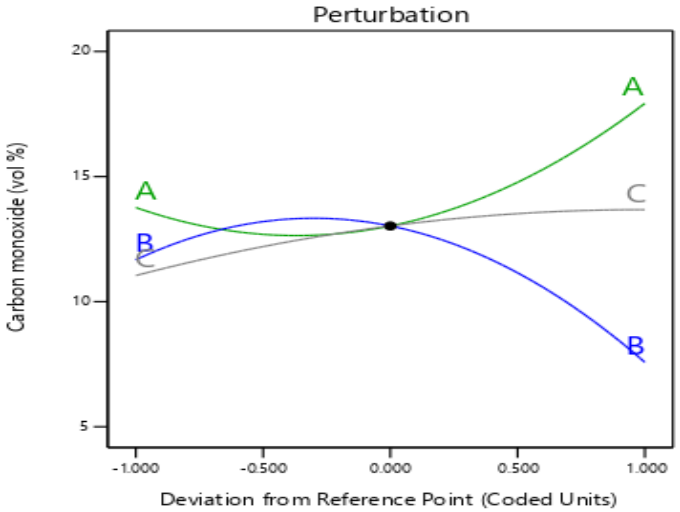

Figure 5: Perturbation Plot of Model Terms (A; Temperature, B; S/B Ratio, and C; Particle Size for CO Produced from Avocado Seed Residue

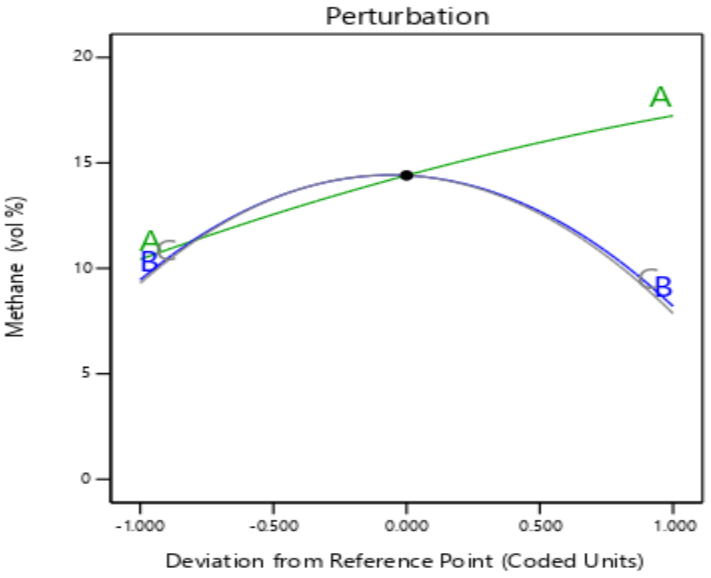

Figure 6: Perturbation Plot of Model Terms (A; Temperature, B; S/B Ratio, and C; Particle Size for CH_4 Produced from Avocado Seed Residue

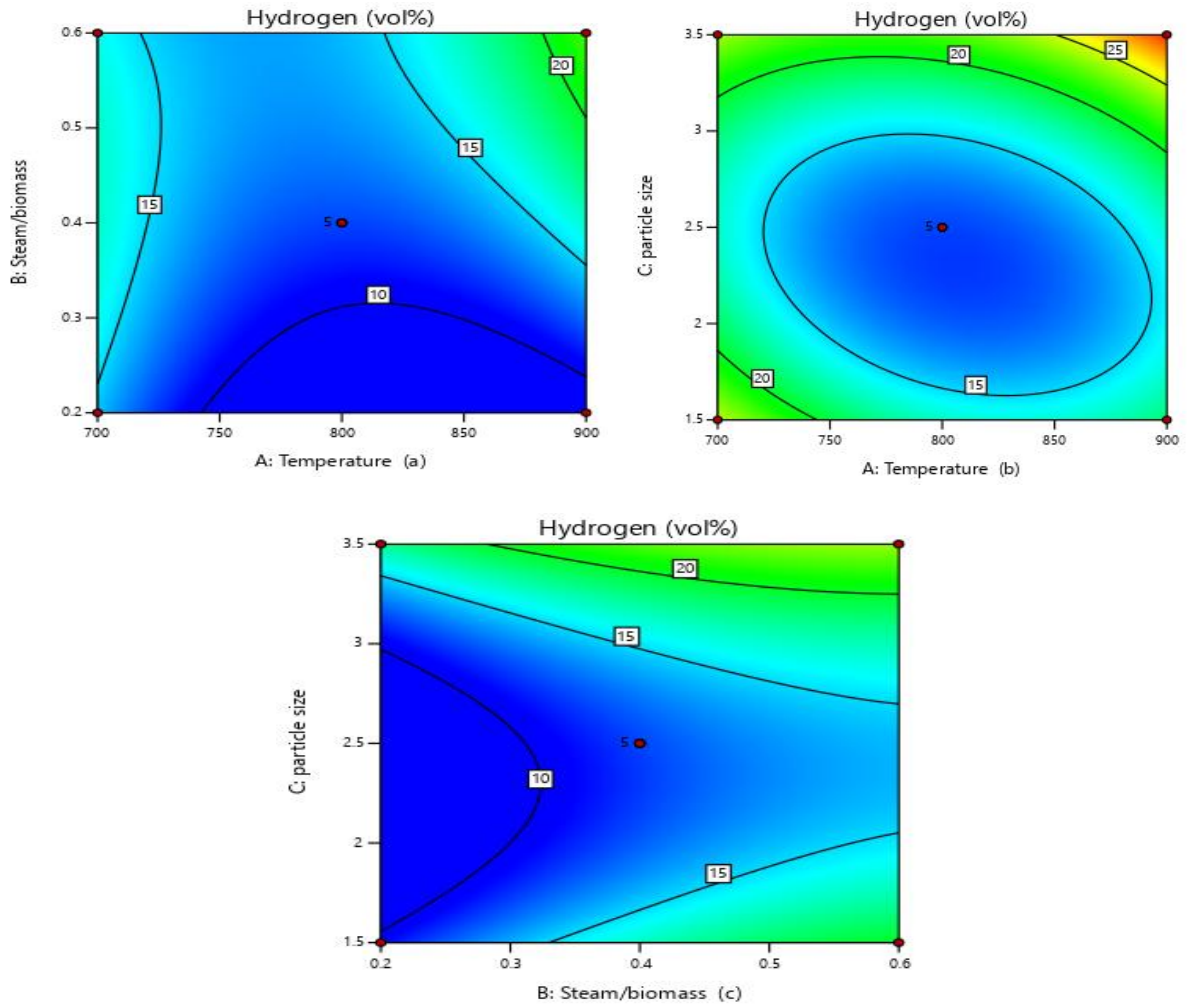

Figure 7: Contour Plots Showing Combined Effects of (a) S/B against Temperature (ºC) (b) Temperature (ºC) against Particle size (mm), and (c) S/B against Particle Size (mm) on the Volume of H_2 Produced from Avocado Seed Residue

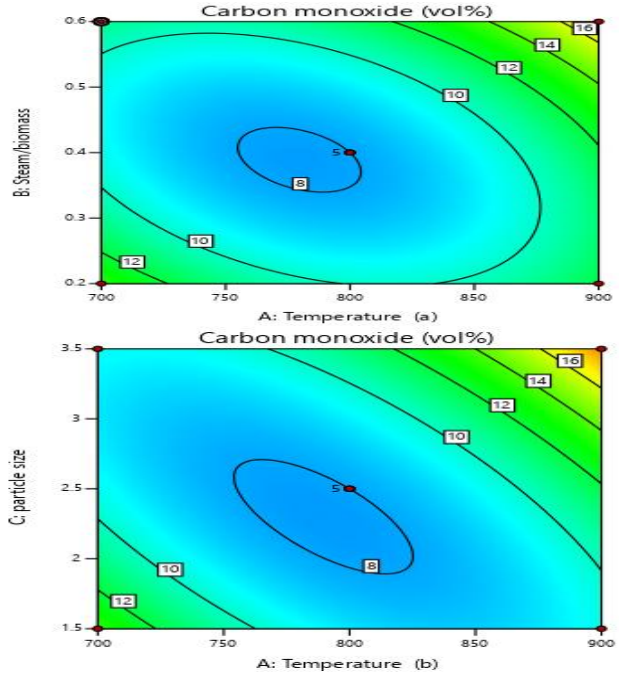

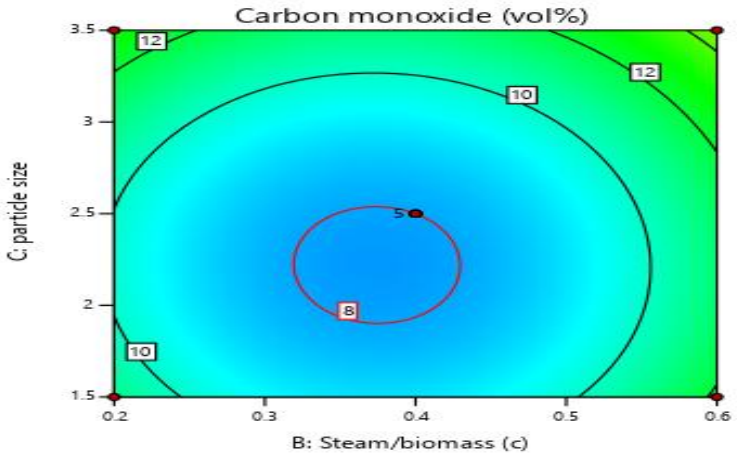

Figure 8: Contour Plots showing Combined Effects of (a) S/B against Temperature (°C) on the Volume of CO Produced, (b) Temperature (°C) against Particle Size (mm), and (c) S/B against Particle Size (mm) on the Volume of CO Produced from Avocado Seed Residue

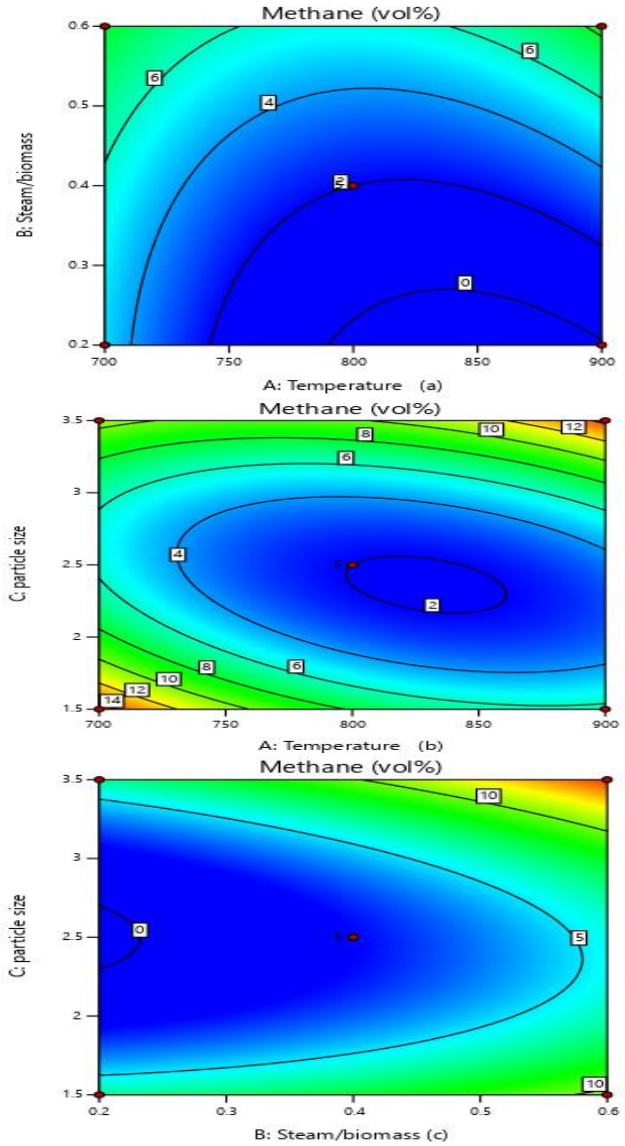

Figure 9: Contour Plots showing Combined Effects of (a) S/B against Temperature (°C), (b) Temperature (°C) against Particle Size (mm), and (c) S/B against Particle Size (mm) on the Volume of CH_4 Produced from Avocado Seed Residue

CONCLUSION

This study reveals that the physicochemical and elemental analyses of ASR possess suitable characteristics for the gasification process. Experiments conducted in a laboratory-scale fluidized-bed reactor demonstrated that hydrogen, carbon monoxide, and methane production are strongly dependent on operating parameters, specifically temperature, steam-to-biomass ratio, and particle size. Application of Box-Behnken Design within the Response Surface Methodology framework enabled the development of robust quadratic models capable of accurately predicting syngas composition, with excellent agreement between predicted and experimental values. The optimal gasification conditions, 900 °C, S/B ratio of 0.60, and a particle size of 2.5 mm, produced maximum yields of hydrogen, carbon monoxide, and methane. These findings, therefore, highlight ASR as a sustainable and effective feedstock for biosyngas generation. Moreover, the study demonstrated that systematic process optimization can substantially improve syngas yield and composition, providing a viable pathway for converting agricultural residues into renewable energy and supporting low-carbon energy solutions.

ACKNOWLEDGEMENT

The authors wish to acknowledge Tetfund for sponsoring the research work through academic staff training and development, Nasarawa State University, Keffi, and the Universiti Putra Malaysia for the laboratories where this work was carried out. We also wish to thank Prof. Irmawati Ramli for her guidance and financial support.

REFERENCES

Abdullah, B., Muhammad, S. A., Shokravi, Z., Ismail, S., Kassim, K. A., Mahmood, A. N., & Aziz, M. M. (2019). Fourth-generation biofuel: A review on risks and mitigation strategies. *Renewable and Sustainable Energy Reviews, 107*, 37–50. https://doi.org/10.1016/j.rser.2019.02.018

Abubakar, M. Ali, Hadiza, Shuaibu & Haruna, Ibrahim (2026). Statistical evaluation and optimisation of biodiesel production from *Gmelina arborea leaf* biomass using calcium hydroxide catalysis under mild conditions. *FUDMA Journal of Sciences*, *10*(2), 94 – 101. DOI: https://doi.org/10.33003/fjs-2026-1003-4746

Adeyemi, A. O., Chiamaka, O., & Oluwatomisin, M. O. (2020). CO_2 emissions and environmental implications in Nigeria. *International Journal of Energy Economics and Policy*, *10*(3), 317–324. https://doi.org/10.32479/ijeep.8050

Adeyemi, A. O., Chiamaka, O., & Oluwatomisin, M. O. (2020). CO_2 emissions and environmental implications in Nigeria. *International Journal of Energy Economics and Policy*, *10*(3), 317–324. https://doi.org/10.32479/ijeep.8050

Ajorloo, M., Ghodrat, M., Scott, J., & Strezov, V. (2022). Recent advances in thermodynamic analysis of biomass gasification: A review on numerical modelling and simulation. *Journal of Energy Institute, 102*, 395–419. https://doi.org/10.1016/j.joei.2022.05.003

Antonio, M., Vincenzo, L., Simeone, C., & Dino, M. (2018). Biofuels production by biomass gasification: A review. *Energies, 11*(811), 1–32. https://doi.org/10.3390/en11040811

Anukam, A. I., Mamphweli, S. N., Reddy, P., & Okoh, O. O. (2016). Characterization and the effect of lignocellulosic biomass value addition on gasification efficiency. *Energy Exploration & Exploitation, 34*(6), 865–880. https://doi.org/10.1177/0144598716665010

Aqsha, A., Tijani, M. M., Moghtaderi, B., & Mahinpey, N. (2017). Catalytic pyrolysis of straw biomasses (wheat, flax, oat and barley) and the comparison of their product yields. *Journal of Analytical and Applied Pyrolysis, 125*, 201–208. https://doi.org/10.1016/j.jaap.2017.03.022

Bayetero, C. M., Yépez, C. M., Cevallos, I. B., & Rueda, E. H. (2022). Effect of the use of additives in biodiesel blends on the performance and opacity of a diesel engine. *Materials Today: Proceedings. Advances in Mechanical Engineering Trends, 49*, 93–99. https://doi.org/10.1016/j.matpr.2021.07.478

Betene, A. D. O., Betene, F. E., Martoïa, F., Dumont, P. J., Atangana, A., & Noah, P. M. A. (2020). Physico-chemical and thermal characterization of some lignocellulosic fibres: *Ananas comosus* (AC), *Neuropeltis acuminatas* (NA) and *Rhecktophyllum camerunense* (RC). *Journal of Minerals and Materials Characterization and Engineering, 8*(4), 205–222.

Bijoy, D., Atmadeep, B., & Amitava, D. (2020). Kinetic modeling of biomass gasification and tar formation in a fluidized bed gasifier using equivalent reactor network (ERN). *Fuel*, 280, 1-15. https://doi.org/10.1016/j.fuel.2020.118582

Bychkov, A. L., Denkin, A. I., Tikhova, V. D., & Lomovsky, O. I. (2017). Prediction of higher heating values of plant biomass from ultimate analysis data. *Journal of Thermal Analysis and Calorimetry, 130*(3), 1399–1405. https://doi.org/10.1007/s10973-017-6350-0

Bychkov, A. L., Denkin, A. I., Tikhova, V. D., & Lomovsky, O. I. (2014). Prediction of higher heating values of lignocellulose from elemental analysis. *Chemistry of Plant Raw Material*, (3), 99–104. https://doi.org/10.14258/jcprm.1403099

Chel-Guerrero, L., Barbosa-Martín, E., Martínez-Antonio, A., González-Mondragón, E. & Betancur-Ancona, D. (2016). Some physicochemical and rheological properties of starch isolated from avocado seeds. *Int. J. Biol. Macromol. 86*, 302–308.

Chinedu, M. Nwachukwu, A. & Toffolo, E.W. (2020). Biomass-based gas use in the Swedish iron and steel industry – Supply chain and process integration considerations. *Renewable Energy, 146*, 2797-2811, https://doi.org/10.1016/j.renene.2019.08.100

Danish, M., Naqvi, M., Farooq, U., & Naqvi, S. (2015). Characterization of South Asian agricultural residues for potential utilization in future energy mix. *Energy Procedia, 75*, 2974–2980. https://doi.org/10.1016/j.egypro.2015.07.604

Ezealigo, U. S., Ezealigo, B. N., Kemausuor, F., Achenie, L. E. K., & Onwualu, A. P. (2021). Biomass valorization to bioenergy: Assessment of biomass residues' availability and bioenergy potential in Nigeria. *Sustainability, 13*, 13806. https://doi.org/10.3390/su132413806

Font Palma, C. (2023). Modelling of tar formation and evolution for biomass gasification: A review. *Applied Energy,*

111, 129–141. https://doi.org/10.1016/j.apenergy.2013.04.082

Gagliano, A., Nocera, F., Bruno, M., & Cardillo, G. (2017). Development of an equilibrium-based model of gasification of biomass by Aspen Plus. *Energy Procedia*, *111*, 1010–1019. https://doi.org/10.1016/j.egypro.2017.03.264

Gillespie, G. D., Everard, C. D., Fagan, C. C., & McDonnell, K. P. (2013). Prediction of quality parameters of biomass pellets from proximate and ultimate analysis. *Fuel*, *111*, 771–777. https://doi.org/10.1016/j.fuel.2013.05.002

Halim, N. H. A., Saleh, S., & Samad, N. A. F. A. (2019). Optimization of oil palm empty fruit bunch gasification temperature and steam to biomass ratio using response surface methodology. *IOP Conference Series: Materials Science and Engineering*, *702*, 012006. https://doi.org/10.1088/1757-899X/702/1/012006

Hamad, M. A., Radwan, A. M., Heggo, D. A., & Moustafa, T. (2016). Hydrogen rich gas production from catalytic gasification of biomass. *Renewable Energy*, *85*, 1290–1300. https://doi.org/10.1016/j.renene.2015.07.082

Hou J., & Zhang J. Robust optimization of the efficient syngas fractions in entrained flow coal gasification using Taguchi method and response surface methodology. International Journal of Hydrogen Energy, 2017, 42(8): 4908-4921. https://doi.org/10.1016/j.ijhydene.2017.01.027

Inayat, M. , S.A. Sulaiman, J.C. Kurnia, Catalytic co-gasification of coconut shells and oil palm fronds blends in the presence of cement, dolomite, and limestone: parametric optimization via Box Behnken Design, J. Energy Inst. 92 (2019) 871–882, https://doi.org/10.1016/j.joei.2018.08.002.

Inayat, M., Sulaiman, S. A., Bhayo, B. A., & Shahbaz, M. (2020). Application of response surface methodology in catalytic co-gasification of palm wastes for bioenergy conversion using mineral catalysts. *Biomass and Bioenergy*, *132*, 105418. https://doi.org/10.1016/j.biombioe.2019.105418

Jibrin, M. A. S., & Olanrewaju, B. M. (2025). Response surface methodology (RSM): A computational approach for optimization of biodiesel production parameters from different feedstocks. *International Journal of Modelling & Applied Science*, *8*(9), 22–41. https://doi.org/10.70382/caijmasr.v8i9.027

Marcos, F., Carolina, S., Claudia, E.V., Felipe, A., Hugo, V. & Jaime, O.V. (2019). Avocado oil: characteristics, properties, and applications. *Molecules*, *24*, 217. doi:10.3390/molecules24112172

Marwan, A.S., Muhammad, S. H., Faisal, A.S.A., Alyaa, A., Norli, I., Mohd, O. A., & Mardiana, I.A. (2021). A review on non-edible oil as a potential feedstock for biodiesel: physicochemical properties and production technologies. *Royal Society of Chemistry*, *11*, 25018-25037, doi:10.1039/D1RA04311K

Minerva, C. G., María, D.C. Y Eulogio, C. (2020). Avocado-Derived biomass as a source of bioenergy and bioproducts: A review. *Appl. Sci. 10* (8195), 1-29, doi:10.3390/app10228195

Muhammad, S., Al-Ansari, T., Inayat, M., Sulaiman, S. A., Parthasarathy, P., & McKay, G. (2020). A critical review on the influence of process parameters in catalytic co-gasification: Current performance and challenges for a future prospectus. *Renewable and Sustainable Energy Reviews*, *134*, 110382. https://doi.org/10.1016/j.rser.2020.110382

Naveenkumar, R. & Baskar, G. (2021). Process optimization, green chemistry balance, and technoeconomic analysis of biodiesel production from castor oil using a heterogeneous nanocatalyst. Bioresour. *Technol. 320*, 124347. https://doi.org/10.1016/j.biortech.2020.124347

Prakash, A., Akshat, T. & Andrew, H. (2022). Mini review of catalytic reactive flash volatilization of biomass for hydrogen-rich syngas production. *Energy and Fuels*, *36*(9), 4640-4652, https://doi.org/10.1021/acs.energyfuels.2c00268

Preeti, Mohod, A. G., Khandetod, Y. P., Dhande, K. G., & Sawant, P. A. (2024). Physico-chemical characterization of coconut shell (*Cocos nucifera*). *International Journal of Advanced Biochemistry Research*, *8*(3), 118–122. https://doi.org/10.33545/26174693.2024.v8.i3Sb.703

Sango, T., Cheumani Yona, A. M., Duchatel, L., Marin, A., Kor Ndikontar, M., Joly, N., & Lefebvre, J.-M. (2018). Stepwise multiscale deconstruction of banana pseudo–stem (*Musa acuminata*) biomass and morpho–mechanical characterization of extracted long fibers for sustainable applications. *Industrial Crops and Products*, *122*, 657–668. https://doi.org/10.1016/j.indcrop.2018.06.05

Savannah, B. (2021). Climate, environmental, and health impacts of fossil fuels. *Environmental and Energy Study Institute (EESI).* Retrieved from https://www.eesi.org/fuels.htm

Seçer, A., & Hasanoglu, A. (2020). Evaluation of the effects of process parameters on co-gasification of Çan lignite and sorghum biomass with response surface methodology: An optimization study for high yield hydrogen production. *Fuel*, *259*, 116230. https://doi.org/10.1016/j.fuel.2019.116230

Serrano, C., Monedero, E., Lapuerta, M., & Portero, H. (2011). Effect of moisture content, particle size and pine addition on quality parameters of barley straw pellets. *Fuel Processing Technology*, *92*, 699–706. https://doi.org/10.1016/j.fuproc.2010.11.031

Sezer, S., & Ozveren, U. (2021). Investigation of syngas exergy value and hydrogen concentration in syngas from biomass gasification in a bubbling fluidized bed gasifier by using machine learning. *International Journal of Hydrogen Energy*, *46*, 20377–20396. https://doi.org/10.1016/j.ijhydene.2021.03.184

Shahbaz, M., Yusup, S., Inayat, A., Patrick, D. O., & Pratama, A. (2016). Application of response surface methodology to investigate the effect of different variables on conversion of palm kernel shell in steam gasification using coal bottom ash. *Applied Energy*, *184*, 1306–1315. https://doi.org/10.1016/j.apenergy.2016.05.045

Sharma, P. B., Gupta, M., Pandey, K., Singh, B., & Baredar, P. (2021). Downdraft biomass gasification: A review on concepts, designs, analysis, modelling and recent advances.

Materials Today: Proceedings, *46*, 5333–5341. https://doi.org/10.1016/j.matpr.2020.08.789

Singh, H., Sapra, P. K., & Sidhu, B. S. (2013). Evaluation and characterization of different biomass residues through proximate and ultimate analysis and heating value. *Asian Journal of Engineering and Applied Technology*, *2*(2), 6–10.

Solal, S. D., Nana, S. A. D., Francis, A. K., & Joseph, K. Y. (2022). A review of response surface methodology for biogas process optimization. *Cogent Engineering*, *9*(1), 211528. https://doi.org/10.1080/23311916.2022.211528

Thomson, R., Kwong, P., Ahmad, E., & Nigam, K. D. P. (2020). Clean syngas from small commercial biomass gasifiers: A review of gasifier development, recent advances and performance evaluation. *International Journal of Hydrogen Energy*, *45*, 21087–21111. https://doi.org/10.1016/j.ijhydene.2020.05.160

Umar, H. A., Sulaiman, S. A., Meor Said, M. A., Gungor, A., & Ahmad, R. K. (2021). Use of response surface methodology to measure the impact of operating variables on the co-gasification of oil palm biomass. *Journal of Hunan University*, *48*(4), 147–157.

Varank, G., Ongen, A., Guvenc, S. Y., Ozcan, H. K., Ozbas, E. E., & Can Güven, E. (2021). Modeling and optimization of syngas production from biomass gasification. *International Journal of Environmental Science and Technology*, 1–15. https://doi.org/10.1007/s13762-021-03374-3

Wang, X., Yang, Z., Liu, X., Huang, G., Xiao, W., & Han, L. (2020). The composition characteristics of different crop straw types and their multivariate analysis and comparison. *Waste Management*, *110*, 87–97. https://doi.org/10.1016/j.wasman.2020.05.018

Wang, Z., He, T., Qin, J., Wu, J., Li, J., Zi, Z., Liu, G., Wu, J., & Sun, L. (2015). Gasification of biomass with oxygen-enriched air in a pilot scale two-stage gasifier. *Fuel*, *150*, 386–393. https://doi.org/10.1016/j.fuel.2015.02.056